
Design of solar powered high step up non-isolated converter with low switching stress

B. Nagi Reddy^{1,*}, B. Poojitha¹

¹Department of EEE, Vignana Bharathi Institute of Technology, Hyderabad, India

*Email: nagireddy208@gmail.com

Abstract

This article proposes a design of solar powered high step up non-isolated converter with low switching stress. The proposed circuit is designed by merging the traditional switched-inductor (SI) boost converter with a boosting cell. The design of new non-isolated boost DC-DC converter is made to control the DC output of the renewable systems particularly for solar. The proposed converter has various benefits such as providing a high efficiency, simplified control, low voltage stress on the active switches and high step-up voltage gain, which makes it suitable for solar energy applications. Additionally, the suggested configuration enables the shared ground connection between supply and load. The performance of the modified non-isolated converter is evaluated under steady state conditions. Operation principles of the suggested topology are shown in detail. To confirm the effectiveness, the theoretical analysis of proposed topology is verified by simulation result. The converter achieved 96% efficiency for the proposed design.

Keywords. DC-DC converter, solar, continuous input current, low stresses, high voltage gain.

1. INTRODUCTION

The challenges of climate change and global warming, both of which are caused by the vastly growing emissions of greenhouse gases, have evolved into significant concerns in the modern world. Photovoltaic (PV) cells, fuel cells, and wind turbines are examples of renewable energy generating technologies that have recently gained favour as potential alternatives. Car high-intensity discharge lights, power supplies, hybrid automobiles, and telecom power systems are just a few examples [1] of the many applications for these lamps. It is possible for a basic boost circuit to attain a boundless voltage gain when the duty ratio is set to 1. Only in theory can this happen. There are large conduction losses in the controlled switch and diode reverse recovery losses due to high duty cycles [2]. Furthermore, the voltage stress of switch is rather high, which indicates that the switch voltage stress is same as the output voltage. It is possible to get a large voltage gain in flyback,

forward, half & full bridges, and push-pull topologies by increasing the number of turns on the transformer [3]. Flyback, complete bridge, and push-pull are other forms of isolated converters.

There are, however, several difficult issues, such as the secondary transformer winding leakage inductance and parasitic capacitance, high spikes in voltage and current, and greater voltage stress on the switching electronics. These issues worsen the system's performance by increasing switching losses due to excessive power dissipation and noise [4]. The switching devices can also be damaged by large voltage spikes, which are also present. By altering the connected inductor's turn's ratio, coupled inductors-based dc-dc converters may also achieve significant voltage gains [5]. They are very easy to manage. This may be accomplished by changing the connected inductor's turn ratio correctly. Voltage spikes occur across the power switches when many inductors are coupled together. In addition to this, the losses caused by leakage inductance bring the converter efficiency down. Because of this, more snubber circuits are necessary, which results in more complicated circuitry [6]. To produce high voltage gain, boost converters can also be used in a cascading or quadratic configuration [7]. In this configuration, two or more boost converters are cascaded together. Cascading boost converters, on the other hand, increase the number of stages, which necessitates a larger board area to house the increased number of switches and gate driver circuits, resulting in a lower power density. Cascading boost converters also increase the size of the board.

When employing many stages, the voltage gain may be enhanced. However, this results in a rise in the total number of circuit components, which leads to more complicated power and control circuits. In addition, the price of the circuit is huge, and its efficiency drops as the aggregate of steps needed to reach a greater voltage grows. In this paper, a novel transformer-less boost converter (TBC) is developed to lower the voltage between switches while still achieving wide step-up voltage. The proposed converter has various benefits such as providing a high efficiency, simplified control, low switching voltage stress on the devices and high step-up voltage gain, which makes it appropriate for solar energy applications [8]. Because of this, the suggested converter requires a lower number of diodes than the traditional SI boost circuit does. This is because the two active switches in the given configuration evenly divide the entire output voltage, which in turn halves the voltage stress that is placed on the switches. So, switches rated for low voltage could be used in the design of the proposed TBC structure. In addition, by employing TBC, a greater voltage gain may be accomplished without an increase in the number of components used in the present SI boost circuit. Also, the converter that was suggested can connect both the load and the supply to a single ground.

2. PROPOSED TBC CONVERTER

Wide voltage gains than standard boost converter may be achieved by utilising SI boost circuit, which incorporates extra switching circuitry. When the

voltage gain is raised, however, it causes a large rise in voltage stress on the switches, which leads to a greater development of total output voltage on the switch. With two switches, voltage stress on the switches is minimised in a transformer less active switched inductor circuit. The converter, on the other hand, can only handle floating loads. Figure 1 depicts the circuitry of TBC, a suggested solution to address these limitations. Lower stress on the switches and a larger voltage gain are achieved by using the TBC. Modifying the SIBC's power circuitry is all that is required to create the circuitry. Two diodes D_a and D_b , active switches S_a and S_b , two capacitors C_a and C_b , two inductors L_a and L_b with identical ratings (L), and a load R make up the proposed TBC circuitry. The traditional SI boost circuit's intermediate diodes have been replaced with a capacitor and an active switch. A parallel charging and sequential discharging of energy components are used in the suggested TBC. A series discharge is used to charge the output filter capacitor when the power is turned off, while a parallel discharge is used to charge the other side of the capacitor when it is turned on.

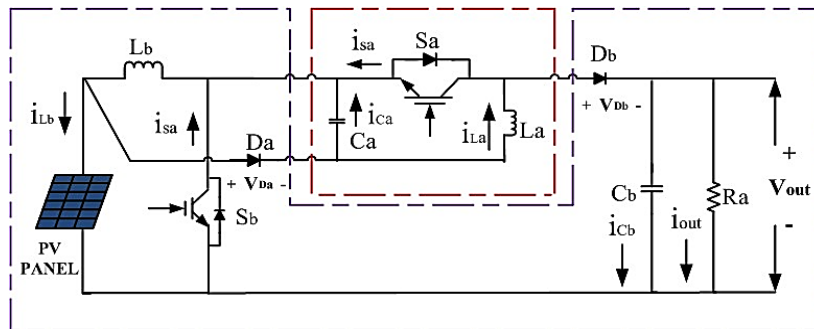


Figure 1. Designed TBC Converter

As a result of this, the suggested TBC reduces the voltage stress on the two active switches to half of what it would otherwise be. This means that the proposed TBC's power circuitry may make use of switches with low voltage ratings. Despite the fact that TBC has the same number of components as a SIBC converter, it has a larger voltage gain. Using this suggested circuit

$$L_a = L_b = L \quad (1)$$

The internal resistance of semiconductor devices and inductors, as well as a capacitor that is very big to maintain a stable voltage, are ignored while studying the characteristics of the circuit's continuous conduction mode (CCM). Time t_0-t_A is the switching duration for mode I in fig. 2 and 3, respectively, which illustrates characteristic TBC waveforms in CCM mode (i.e., ON period).

2.1 Basic operation

There are two modes of CCM operation for the suggested TBC: one in which both switches are on, and one in which both switches are off.

Mode I (Period t_0-t_A): -As seen in figure 2, mode I of TBC has an analogous circuit. Switch S_b charges inductor L_b , while input supply (V_{PV}) charges inductor L_a via diode D_a and switches S_a and S_b , while input supply (V_{PV}) charges capacitance C_a via diodes D_a and switch S_b . Note that the energy elements L_a , L_b , and C_a , are charged in the parallel-paths and the output filter capacitor C_b discharges through a load. In this mode, diode D_a is in forward bias and D_b is in reverse bias. Inductors and capacitors have voltages and currents that may be stated as

$$v'_L = v'_{L_a} = v'_{L_b} \approx V_{PV}, v'_{C_b} = V_0 \quad (2)$$

$$i'_{PV} = i'_{L_a} + i'_{L_b} + i'_{C_a}, i'_{C_b} = -i_0 \quad (3)$$

In this case, the superscript is mode I and the subscript are the element.

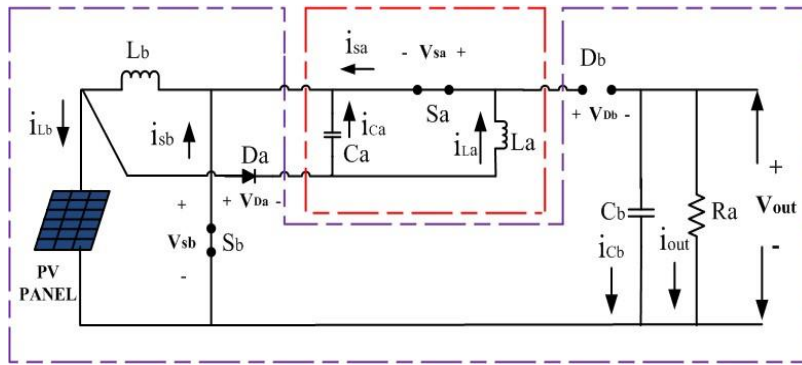


Figure 2. Mode 1 operation of TBC topology

Mode II (Period t_A-t_B): - TBC mode II comparable circuit is shown in Figure 3. The energy elements L_a , L_b , and C_a , are charged in the series-path with the supply voltage V_{PV} ; electrical power is provided to the load resistance through a diode for the time being the filter capacitor C_b charges. Diode D_a will be reverse biased and D_b is in forward bias, in this stage. Voltages and currents that may be stated as

$$v''_L = v''_{L_a} = v''_{L_b} \approx V_{PV} - \frac{V_0}{2}, v''_{C_b} = V_0 \quad (4)$$

$$i''_{PV} = i''_{L_a} = i''_{L_b} = i''_L, i''_{C_b} \approx i''_L - i_0 \quad (5)$$

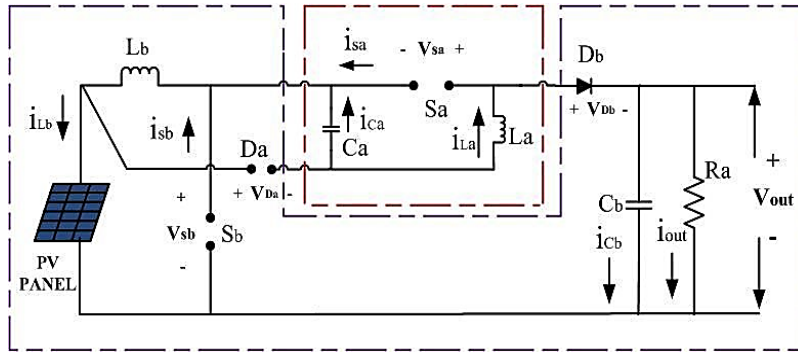


Figure 3. Mode 2 operation of TBC topology

Mode II is represented by a superscript and a lowercase subscript, respectively. The voltage gain of TBC may be written as follows using the inductor volt second balancing principle:

$$\frac{V_o}{V_{PV}} = \frac{2}{1-d} \quad (6)$$

where V_G and d are the voltage gain and duty ratio, respectively. It is clear from equation (6) that the voltage gain of the TBC is superior to that of the traditional converters.

2.2 Inductors design

$$L_a = L_b = \frac{DV_{PV}}{f_s \Delta I_{La}} \quad (7)$$

For $D = 0.6$, $V_{PV} = 24V$, $f_s = 60 \text{ kHz}$ and $\Delta I_{a\&b} = 0.5$, the values of L_a & L_b are given by L_a & $L_b = 480 \mu\text{H}$.

2.3 Capacitors design

$$C_a = \frac{P_{in}(1-D)}{V_{in}f_s \Delta V_{Ca}} \quad (8)$$

$$C_b = \frac{P_o D}{f_s \Delta V_{Cb} V_o} \quad (9)$$

For $D = 0.6$, $V_o = 120V$, $f_s = 60 \text{ kHz}$ and $\Delta V_{Ca} = 2A$, $\Delta V_{Cb} = 1A$. The value of C_a , C_b are given by $C_a = 27.78 \mu\text{F}$, $C_b = 16.67 \mu\text{F}$.

3. SIMULATION RESULTS

The projected converter is designed for an output power of 200W, with an output voltage of 120V. With the input voltage of 24V, the required output voltage

with a gain of 5, can be produced at a duty ratio of 60%. The load resistance is calculated using basic formula as 72Ω . To reduce the converter size, it is advisable to take higher switching frequencies (f_s), however for the proposed simulation and design 60 kHz frequency is considered. The proposed converter contains four energy elements which includes two inductors and two capacitors. With the considerable current and voltage ripples on the inductors and capacitors respectively, the energy component values are calculated and are observed in table 1. Figure 4 represents the input DC voltage waveform along with the input current plotted using MATLAB simulation. A 24V DC input voltage is considered as the output of fuel cell to design the proposed converter which can be observed in fig. 4. Similarly, it can be observed that the input current waveform is continuous and it has a ripple of 5A.

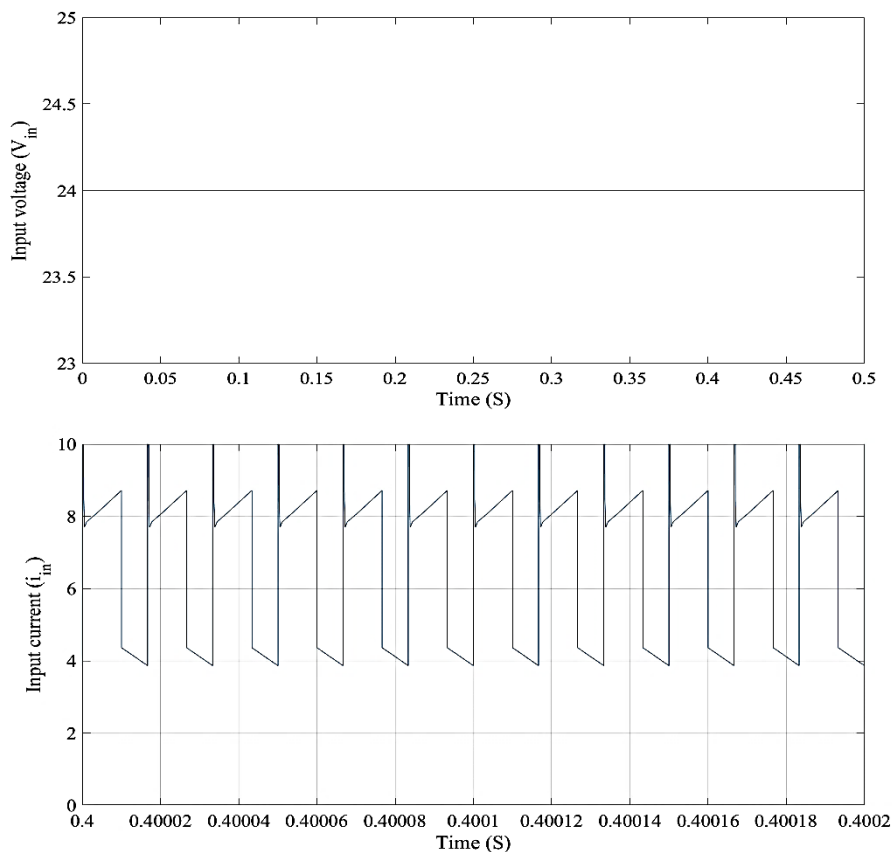


Figure 4. Simulated waveform of the input DC voltage with a voltage 24V and continuous input current with 5 A ripple as considered for design

The simulated voltage waveform of capacitor 1 (C_1) is shown in fig. 5. The charging and discharging phenomenon can be observed in the simulation results (fig. 5), with a considerable peak ripple of 2V.

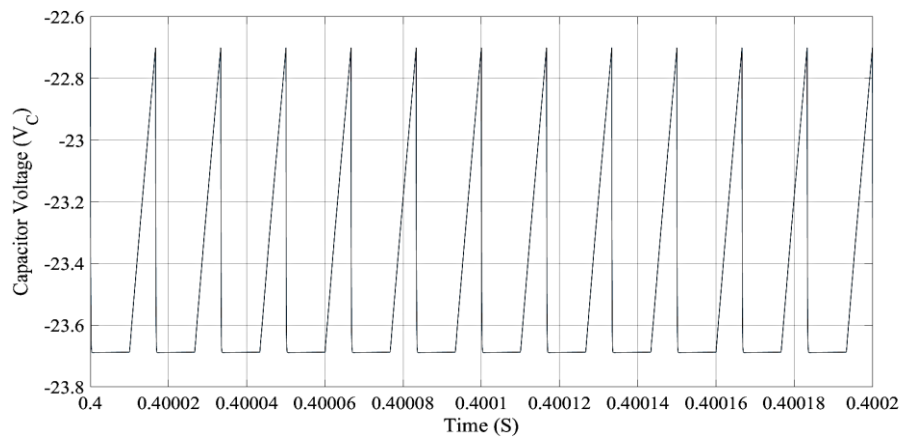


Figure 5. Simulated waveform of the capacitor 1 voltage with a peak ripple of 2V

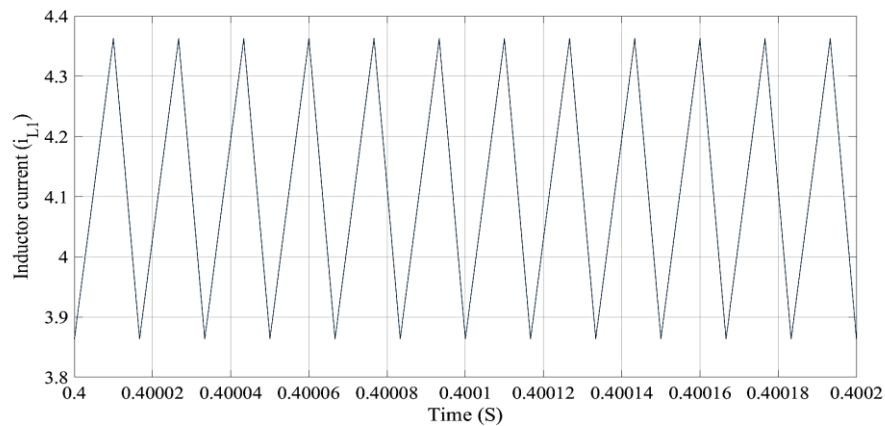


Figure 6. Inductor 1 (L_1) current waveform with a peak-to-peak ripple of 0.5 A

Figures 6 & 7 shows the simulated inductor current waveforms i_{L1} & i_{L2} respectively under steady state operation (for 10 cycles). From fig. 6 it can be noted that the inductor L_1 peak to peak ripple approximately 0.5A. This value is exactly matches to the theoretical consideration of inductor L_1 design. From fig. 7 it can be noted that the inductor L_2 peak to peak ripple approximately 0.5A. This value is exactly matches to the theoretical consideration of inductor L_2 design. Finally, the simulated output waveforms are shown in the figs. 8 & 9 of the proposed converter. The DC output current can be given as 1.6667A theoretically. The simulated value is approximately 1.63A and is much closer to the theoretical value. Figure 9 represents the simulated DC output voltage with very low ripple ($< 0.5\%$ approximately). The simulated value is 118V, much closed to the theoretical value.

As mention above, the output power can be calculated as 192.34W for the 200W design and the voltage stresses of diode 1 voltage is 60V and d2 is 120V. Hence the efficiency is 96.13.

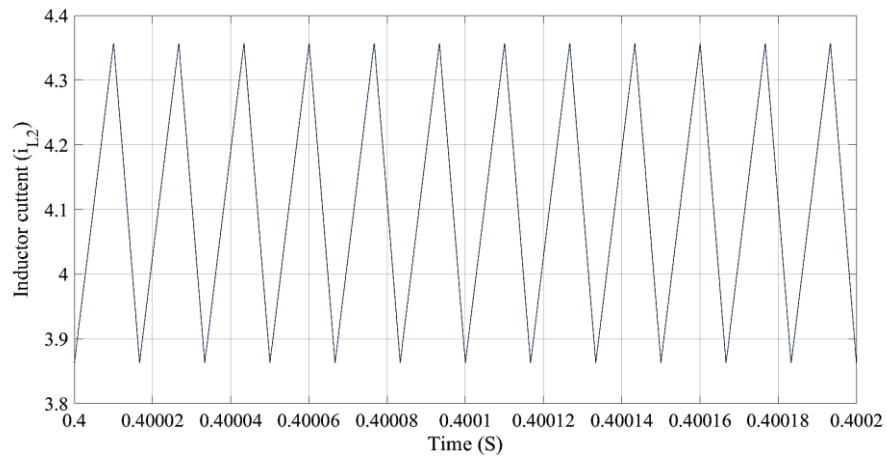


Figure 7 Inductor 2 (L_2) current waveform with a peak-to-peak ripple of 0.5 A

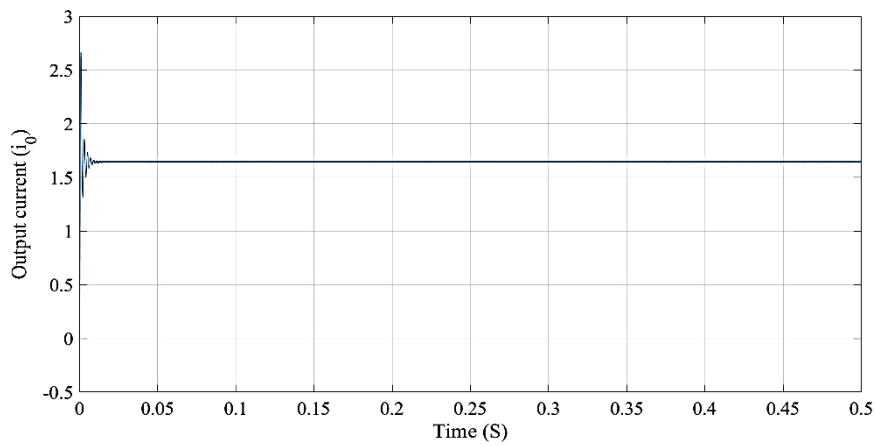


Figure 8. DC output current waveform of proposed topology

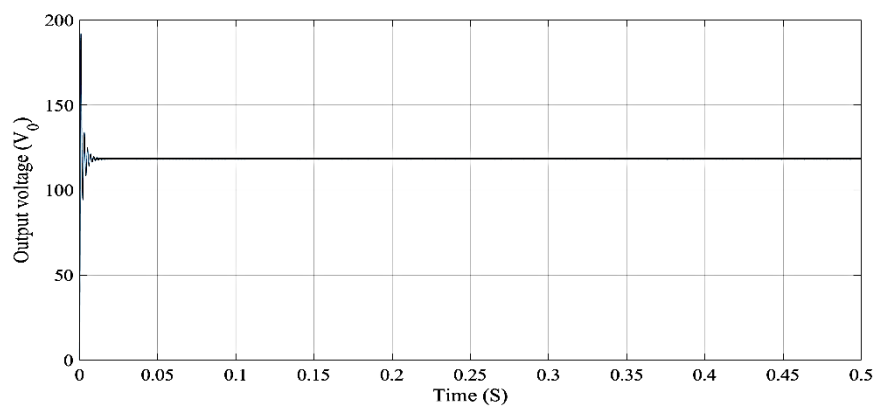


Figure 9. Output DC voltage waveform of proposed topology

4. CONCLUSION

A new TBC configuration was proposed for step-up applications with less voltage stress across the switch. Traditional SIBC required exactly the same number of components as SI boost circuit. When compared to a standard boost network and a SIBC, TBC's voltage gain was significantly higher. As compared to a standard converter, this converter used half as many diodes and experienced half the output voltage stress. As a result, active switches with low voltage ratings might be used in the TBC system. There was a discussion of the CCM mode's operation, including its voltage gain. Switches with lower voltage ratings have been shown to provide a larger voltage gain. Only diode D_a and switch S_b were used to link capacitance in Mode I of the proposed converter architecture to input supply in Mode II.

REFERENCES

- [1] B. Sri Revathi and M. Prabhakar, "Non isolated high gain DC-DC converter topologies for PV applications – a comprehensive review," *Renewable Sustain. Energy Rev.*, vol. 66, pp. 920–933, Dec. 2016.
- [2] M. S. Bhaskar, S. Padmanaban, and F. Blaabjerg, "A multistage DC-DC step-up self-balanced and magnetic component-free converter for photovoltaic applications: Hardware implementation," *Energies*, 10 (5), May 2017.
- [3] S. Padmanaban, M. S. Bhaskar, P. K. Maroti, F. Blaabjerg, and V. Fedák, "An original transformer and switched-capacitor (T & SC)-Based extension for DC-DC boost converter for high-voltage/low-current renewable energy applications: Hardware implementation of a new t & SC boost converter," *Energies*, vol. 11, no. 4, Apr. 2018, Art. no. 783.
- [4] R. Suryadevara and L. Parsa, "Full-bridge ZCS-converter-based high gain modular DC-DC converter for PV integration with medium-voltage DC grids," *IEEE Trans. Energy Convers.*, vol. 34 (1), pp. 302–312, Mar. 2019.
- [5] Y. Chen, Z. Lu, and R. Liang, "Analysis and design of a novel high-step-up DC/DC converter with coupled inductors," *IEEE Trans. Power Electron.*, vol. 33, no. 1, pp. 425–436, Jan. 2018.
- [6] R. Moradpour, H. Ardi, and A. Tavakoli, "Design and implementation of a new SEPIC-Based high step-up DC/DC converter for renewable energy applications," *IEEE Trans. Ind. Electron.*, 65 (2), pp. 1290–1297, Feb. 2018.
- [7] S. Lee and H. Do, "Quadratic boost DC-DC converter with high voltage gain and reduced voltage stresses," *IEEE Trans. Power Electron.*, 34 (3), pp. 2397–2404, Mar. 2019.
- [8] Nagi reddy. B, Sahithi Priya. Kosika, Manish Patel. Gaddam, jagadhishwar. Banoth, Ashok. Banoth, Srikanth goud. B, "Analysis of positive output buck boost topology with extended conversion ratio", *Journal of Energy Systems*, 6(1), pp. 62–83, 2022.